

Electron energy-loss fine structure of a polycrystalline titanium surface

This article has been downloaded from IOPscience. Please scroll down to see the full text article.

1995 J. Phys.: Condens. Matter 7 37

(<http://iopscience.iop.org/0953-8984/7/1/005>)

View [the table of contents for this issue](#), or go to the [journal homepage](#) for more

Download details:

IP Address: 171.66.16.179

The article was downloaded on 13/05/2010 at 11:37

Please note that [terms and conditions apply](#).

Electron energy-loss fine structure of a polycrystalline titanium surface

Mitsunori Kurahashi, Masahiro Yamamoto, Mahito Mabuchi and Shizuo Naito

Institute of Atomic Energy, Kyoto University, Uji, Kyoto 611, Japan

Received 3 October 1994

Abstract. The temperature dependence of the electron energy-loss fine structure (EELFS) of a polycrystalline titanium surface has been measured in reflection mode for electron beams at different incidence angles to the normal of the surface. We have found that within experimental error (about 0.06 Å) the interatomic distance between titanium atoms remains unchanged as the depth from the surface changes and that the EELFS Debye–Waller factor has larger values for larger incidence angles. This result is compared with the reported results of LEED measurements.

1. Introduction

The electron energy-loss fine structure (EELFS) is a feature observed at an energy above the core loss edge in electron energy-loss spectra. In recent years it has been experimentally and theoretically demonstrated that the EELFS observed in both transmission mode and reflection mode can be analysed using a formalism similar to that used for the analysis of the extended x-ray absorption fine structure (EXAFS) [1–7]. Since the reflection EELFS preferentially gives us information about a surface region owing to the short mean free path of a probe electron, it has been applied to the analysis of surface structures [5, 7–13] and surface vibrational properties [13–15], which can be discussed in terms of the radial distribution function (RDF) or the EELFS Debye–Waller factor (DWF). In comparison to LEED, which has been widely used for surface structural analysis, EELFS is particularly useful in that it does not require a single-crystal sample and it gives us information about the particular local environment around the atomic species excited by incidence electrons.

Characteristic behaviours in surface layers of solids, such as the surface relaxation or the enhanced motion of atoms, are expected to be well investigated via the analysis of the depth dependence of the EELFS RDF or DWF. This is particularly so when we attempt to make clear the difference between the behaviours in the surface and those in the bulk. However, there are only a few reports on such analysis [13, 15], and to our knowledge no detailed analysis of the depth dependence of the EELFS DWF has been reported. We here consider the EELFS of titanium primarily because it can comparatively easily be measured above the titanium L_{23} edge. Actually measurements of the EELFS of titanium have been reported by some workers [1, 11]. No discussion, however, is found about the change in the EELFS measured for electron beams at different incidence angles, which permits an analysis of the depth dependence of the RDF and the EELFS DWF.

In the present study we measure the temperature dependence of the EELFS of a clean titanium surface at different incidence angles. We discuss the change in the interatomic

distance and the EELFS DWF with the incidence angle and with the depth from the surface. The result is compared with those obtained from the LEED measurements [16, 17].

2. Experimental details

All measurements were done in an ultra-high-vacuum (UHV) system which had a base pressure of the order of 10^{-8} Pa. The electron energy-loss spectra and Auger electron spectra (AES) were obtained by the use of a Varian single-pass cylindrical mirror analyser with resolution (E/dE) of 200. We measured the derivative electron energy-loss spectra using an electron beam with an incident energy E_p of 1800 eV and a current of $1.5 \mu\text{A}$. In order to change the penetration depth of incident electrons, we used the electron beam at four incidence angles $\theta_i = 20^\circ, 60^\circ, 75^\circ$ and 80° to the normal of the specimen surface. The modulation voltage was selected to be 10 V peak to peak. It took less than 15 min for a single scan. To improve the signal-to-noise ratio in the spectra, we repeated the measurement four to five times and numerically averaged the collected data.

A polycrystalline titanium foil of dimensions $25 \text{ mm} \times 25 \text{ mm} \times 0.025 \text{ mm}$ and 99.95% purity was used as a specimen. It was mechanically polished, ultrasonically degreased in acetone and then spot-welded onto two tantalum support wires 0.8 mm in diameter. In order to clean the surface the specimen was heated resistively by passing an AC current through it. After this heat treatment we found no significant difference in the Auger electron spectra of the titanium surface measured at room temperature and at 373–973 K. The temperature of the specimen was measured with a Pt–PtRh13% thermocouple spot-welded to it and was controlled with a thermoregulator. The fluctuation of the specimen temperature was within ± 5 K. The surface of the specimen was again cleaned by repeating Ar^+ ion bombardment ($2 \text{ keV}, 10 \mu\text{A cm}^{-2}$) at 773 K followed by annealing at 1073 K. We continued this procedure until no segregation of sulphur was observed for the specimen heated to 973 K for more than an hour. The cleanliness of the specimen was monitored by AES. When contamination was observed, we momentarily heated the specimen to a high temperature to recover the cleanliness.

We now make a rough estimate of the penetration depth assuming that the probe electron can travel through its attenuation length in titanium metal. The attenuation length for a 1800 eV electron can be estimated to be 23.13 Å by using the formula reported by Seah and Dench [18]. The estimated penetration depth is thus 9.14 Å, 5.89 Å, 3.81 Å and 2.84 Å for $\theta_i = 20^\circ, 60^\circ, 75^\circ$ and 80° , respectively. These values correspond to 3.9, 2.5, 1.6 and 1.2 monolayers with a spacing of 2.34 Å and parallel to the Ti(0001) surface.

3. The method of EELFS data analysis

Figure 1 shows the temperature dependence of the electron energy-loss spectra for the L_{23} edge of the clean titanium surface that were measured at an incidence angle of 20° . The L_{23} edge is located at an energy loss of 460 eV followed by the EELFS oscillation. The EELFS oscillation of the L_{23} edge was found to decay with increasing temperature, while the shape and intensity of the spectrum of the L_{23} edge was found to remain unchanged. The structure at 560 eV is due to the ionization of the L_1 edge and overlaps the EELFS oscillation. In order to minimize the influence of the L_1 edge on the analysis of the EELFS oscillation, we normalize the EELFS spectra with respect to the peak-to-peak intensity of the L_{23} edge and subtract from the EELFS spectra the spectrum measured at 973 K. We can ignore the effect of the L_1 edge on the resulting EELFS spectra for the following reasons.

First, through the process of the subtraction the structure due to the ionization of the L_1 edge is cancelled because its shape and intensity is, as in the case of the L_{23} edge, expected to remain unchanged with temperature. Secondly, the amplitude of the EELFS oscillation that originated from the ionization of the L_1 edge is much weaker than that of the L_{23} edge considering the difference of intensities of their thresholds. In the following, we will demonstrate that the results of our analysis, which ignores the effect of the L_1 edge, agree well with the reported results. This supports the assumption that the effect of the L_1 edge is negligible.

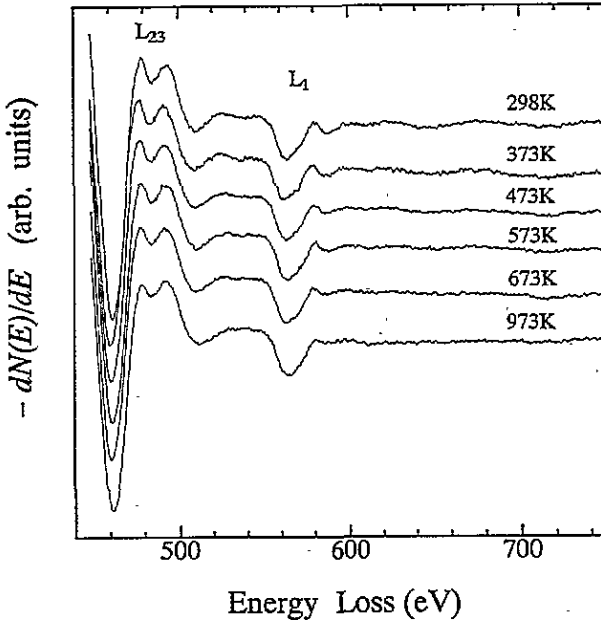


Figure 1. The electron energy-loss spectra of the titanium L_{23} edge measured at the temperatures shown. Measurements were made in first-derivative mode at an incident energy $E_p = 1.8$ keV and the incidence angle $\theta_i = 20^\circ$.

Figure 2 shows the EELFS spectra from which the spectrum measured at 973 K has been subtracted. The EELFS spectra are numerically integrated and the background is removed by fitting to them a sixth-order polynomial curve. The small change in the order of the fitting polynomial curve has little effect on the shape of the modulating structure obtained. The energy loss is graduated with respect to the onset energy of the L_{23} edge (460 eV) and the spectra are then transformed into k -wavevectors. The modulating structure $\chi'_{298}(k)$ is thus isolated and shown in figure 3. The noisy spectrum shown in figure 2 has become the smooth $\chi'_{298}(k)$ curve through the process of numerical integration. The maximum and minimum positions of $\chi'_T(k)$ agree well with those in the reported $\chi(k)$ curves of EXAFS [19] and EELFS [1]. If $\chi_T(k)$ is the EELFS modulating structure at temperature T , then $\chi'_T(k)$ can be written as

$$\chi'_T(k) = \chi_T(k) - \chi_{973}(k). \quad (1)$$

Following the standard method for EXAFS, we multiply the $\chi'_T(k)$ by k and then Fourier transform it in the range $3.3 < k (\text{\AA}^{-1}) < 8.0$ using a Henning window function. Because of the linearity of the Fourier transform, the function $F'_T(R)$ obtained may be written as

$$F'_T(R) = F_T(R) - F_{973}(R) \quad (2)$$

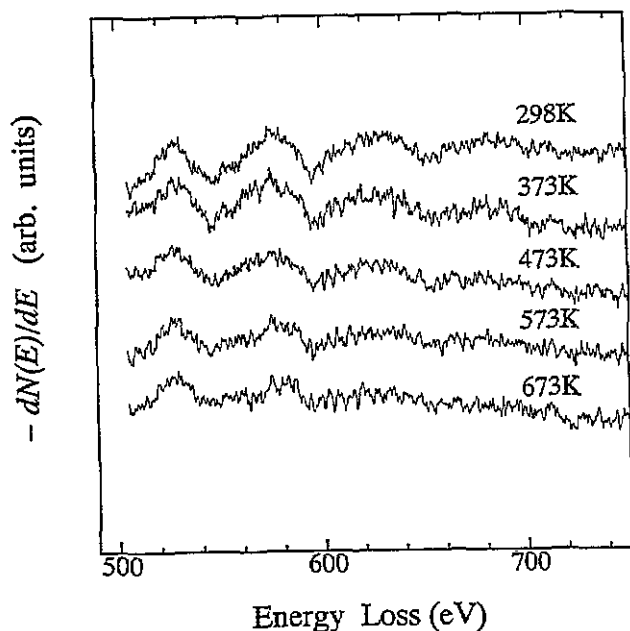


Figure 2. The electron energy-loss spectra with subtraction of the spectrum measured at 973 K. The spectra were measured at $\theta = 20^\circ$ and normalized with respect to the L_{23} edge intensity before performing the subtraction.

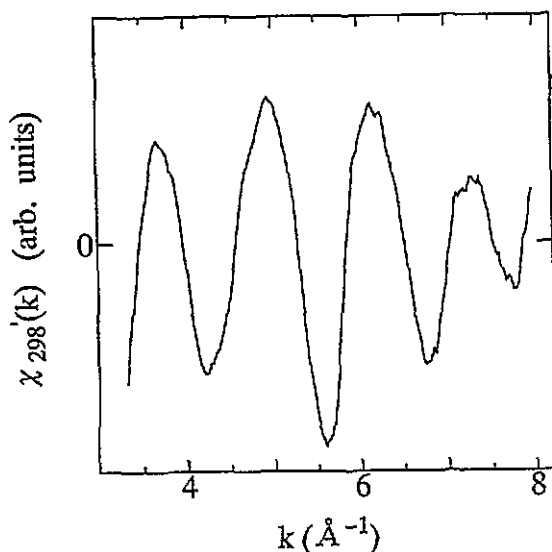


Figure 3. The EELFS structure obtained from the spectra beyond the titanium L_{23} edge measured at 298 K and $\theta_1 = 20^\circ$. The k -wavevector is referred to the L_{23} edge.

where $F_T(R)$ and $F_{973}(R)$ denote the RDF at T and 973 K, respectively. We assume that the difference in the peak positions for $F_{298}(R)$ and $F'_{298}(R)$ is negligibly small. The validity of this assumption can be justified from the discussion of the temperature dependence of the peak position and the intensity of the RDF. First, from the thermal expansion coefficient of

titanium [20] the change in the peak position of $F_T(R)$, i.e. the increase in the interatomic distance, is estimated to be less than 0.02 \AA for temperatures from 298 K to 973 K. Secondly, the intensity of $F_{973}(R)$ is estimated to be less than a third of that of $F_{298}(R)$ from the EELFS DWF evaluated by using Debye approximation. Consequently, the difference is estimated to be less than 0.007 \AA in bulk titanium. In the surface, the difference is expected to be of the same degree for the following reasons: in the surface, the increase in the interatomic distance would be larger than that in the bulk; however, the intensity of $F_{973}(R)$ is estimated to be less than an eighth of that of $F_{298}(R)$ from the same evaluation using the reported surface Debye temperature of Ti(0001) [17].

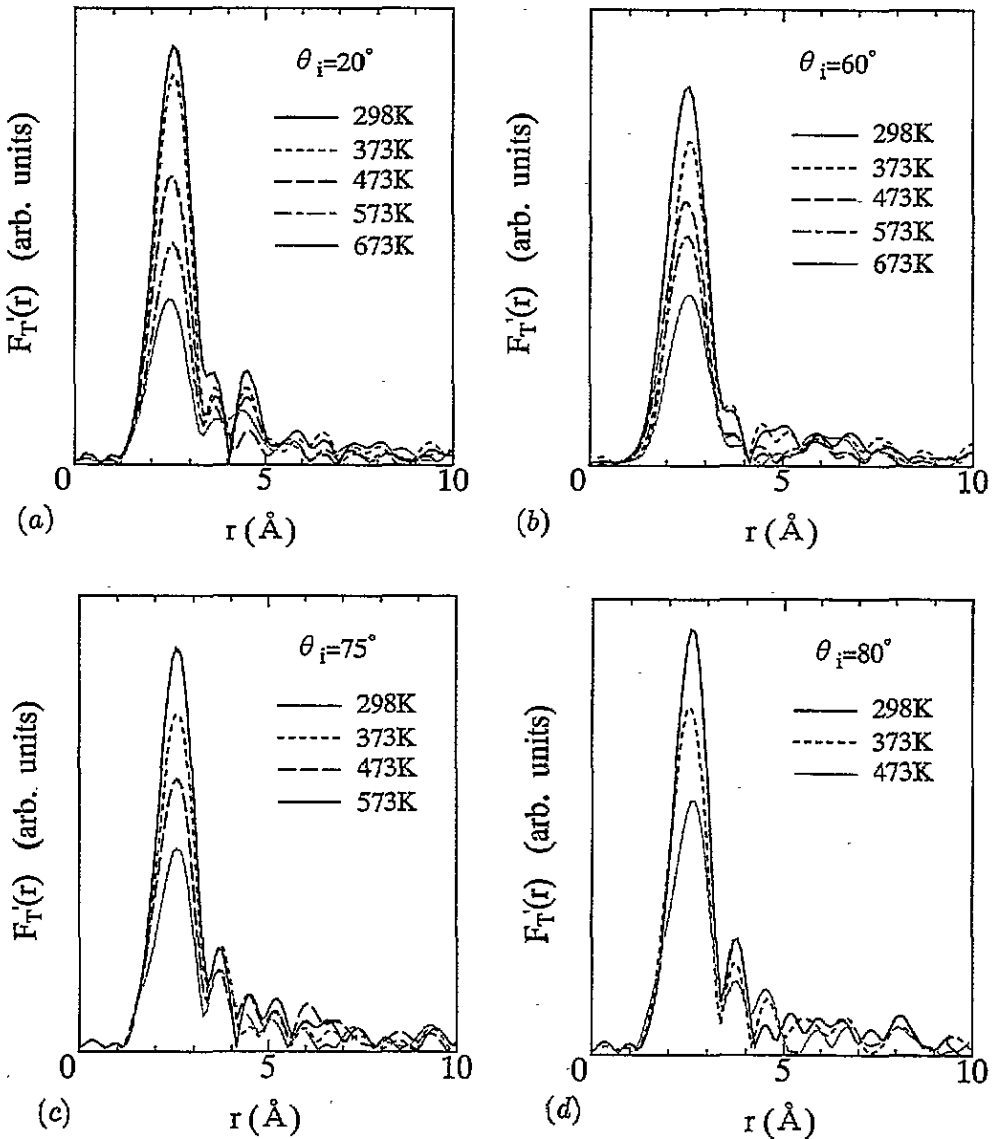


Figure 4. The Fourier transforms $F_T'(R)$ of the EELFS structure $\chi_T'(k)$ obtained from the spectra measured at (a) $\theta_i = 20^\circ$, (b) $\theta_i = 60^\circ$, (c) $\theta_i = 75^\circ$ and (d) $\theta_i = 80^\circ$.

In figure 4, (a)–(d), $F_T'(R)$ is shown for $\theta_i = 20^\circ, 60^\circ, 75^\circ$ and 80° . The corresponding penetration depths are about 9.1 Å, 5.9 Å, 3.8 Å and 2.8 Å. For the measurements at $\theta_i = 75^\circ$ above 673 K and at $\theta_i = 80^\circ$ above 573 K, the signal is too strongly attenuated to permit analysis at higher temperatures. The first peak position for $F_{298}'(R)$ is reproducible within 0.06 Å and agreed well with the reported EXAFS [19] and EELFS [1] RDF. The peaks beyond the second-nearest-neighbour shell, however, are affected by the ripple resulting from the Fourier integration within the limited k -range. Therefore we will discuss only the first peak in detail.

4. Results and discussion

No difference in the first peak positions of $F_{298}'(R)$ is found, within the experimental error, for the measurements at different incidence angles. This indicates that the change in the interatomic distance between the nearest-neighbour (NN) titanium atoms is less than 0.06 Å within the depth 9.1 Å from the surface. This result is in good agreement with the LEED result given by Shih *et al* [16]. They showed that the contraction of the interlayer spacing between the outermost layer and the second layer of the Ti(0001) surface was 2% of the interlayer spacing in the bulk and that the interatomic distance between titanium atoms on the outermost layer agreed with that in the bulk. Therefore the contraction in the average distance from an atom on the outermost layer to its NN atoms is estimated to be less than 1% of the interatomic distance, i.e. less than 0.03 Å, provided that only the outermost layer is excited. If the excitation in the second layer is also considered, the resulting contraction is smaller. Since the contribution from the second layer cannot be neglected even for the measurement at $\theta_i = 80^\circ$ in the present study, we expect no appreciable change in the position of the peak corresponding to the NN atoms.

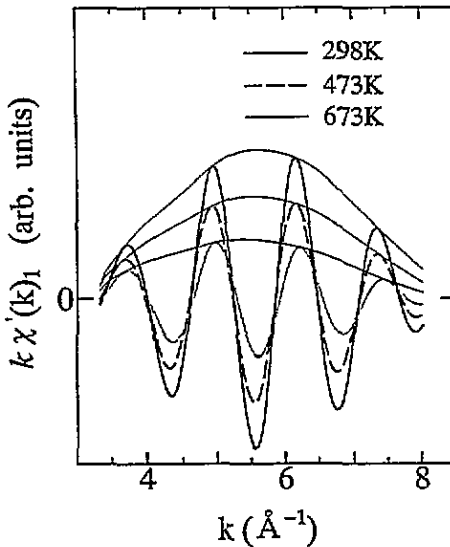


Figure 5. The Fourier-filtered EELFS structures and the corresponding amplitudes obtained from the first peaks of $F_T'(R)$ for 298 K, 473 K, 673 K in figure 4(a).

The temperature dependence of DWF has been determined by a procedure based on the ratio method [21]. In the present study this method has been modified as follows. First,

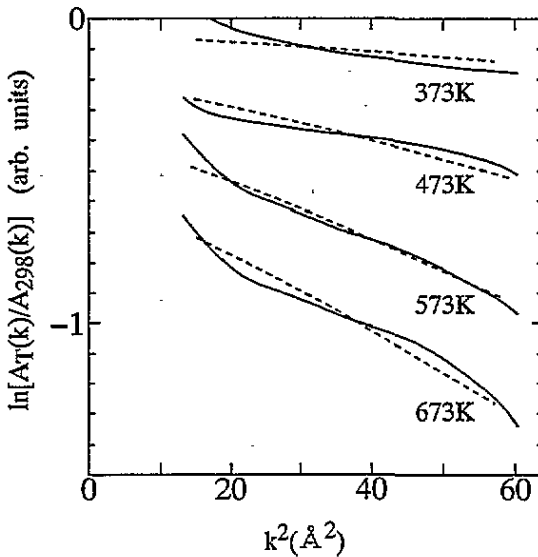


Figure 6. The ratios of the amplitudes at $T = 373$ K, 473 K, 573 K and 673 K to the amplitude at 298 K plotted against k^2 . The amplitudes have been calculated using the spectra measured at $\theta_i = 20^\circ$. The solid lines are calculated from (3) and the dashed lines show the fitting functions.

the contribution of the first coordination shell to the EELFS modulation has been singled out by backtransforming to the k -space the first peak in the RDF. In figure 5, the resulting $k\chi'(k)$ -filtered EELFS function ($k\chi'(k)_1$) and its amplitude function are shown for 298 K, 473 K and 673 K. Via the use of harmonic approximation [22] the amplitude function $A_T(k)$ is found to be proportional to $(\exp[-2\sigma_1^2(T)k^2] - \exp[-2\sigma_1^2(973)k^2])$ because the difference in the NN distances at temperatures T and 973 K is negligibly small as mentioned previously. Here $\sigma_1^2(T)$ is the EELFS DWF for the first coordination shell at temperature T . Since the coordination number does not change with temperature, the amplitude ratio can be reduced to

$$\ln \left[\frac{A_T(k)}{A_{298}(k)} \right] = \ln \left(\frac{\exp[2(\sigma_1^2(973) - \sigma_1^2(T))k^2] - 1}{\exp[2(\sigma_1^2(973) - \sigma_1^2(298))k^2] - 1} \right). \quad (3)$$

Figure 6 shows (3) calculated for 373 K, 473 K, 573 K and 673 K plotted against k^2 . The two parameters $\sigma_1^2(973) - \sigma_1^2(T)$ and $\sigma_1^2(973) - \sigma_1^2(298)$ in (3) have been determined by minimizing the sum of squares of the differences between the values calculated using the experimental result and a fitting function at each temperature. As shown in figure 6, the overall behaviour of the left-hand side of (3) is well reproduced by the fitting function. In the following, we will discuss only $\Delta\sigma^2 \equiv \sigma_1^2(T) - \sigma_1^2(298)$, which is the difference between the two parameters, because the right-hand side of (3) converges to $2(\sigma_1^2(T) - \sigma_1^2(298))k^2$ for large k^2 and only the difference of the two parameters is of significance.

In figure 7, $\Delta\sigma^2$ is plotted for different θ_i -values. The $\Delta\sigma^2$ -value is larger for a larger θ_i , and for $\theta_i = 80^\circ$ it is about twice that for $\theta_i = 20^\circ$. The estimated penetration depth is about 3.9, 2.5, 1.6, and 1.2 monolayers for $\theta_i = 20^\circ, 60^\circ, 75^\circ$ and 80° , respectively. This result indicates that the $\Delta\sigma^2$ -value for the surface layer is much larger than that of the other layers in the polycrystalline titanium. Furthermore, its value can be estimated to be more than twice that for the bulk. In order to compare this result with other experimental results reported, we calculate $\Delta\sigma^2$ using Debye approximation and estimate the Debye temperature

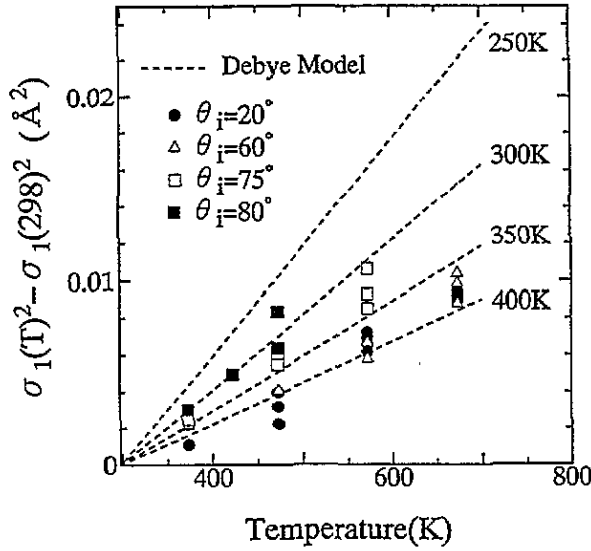


Figure 7. $\Delta\sigma^2 = \sigma_1^2(T) - \sigma_1^2(298)$ for first coordination shell obtained experimentally at the incidence angles shown. The dashed lines show $\Delta\sigma^2$ calculated by using (4) at the θ_D -values shown.

θ_D for different incidence angles. As in the EXAFS DWF, the EELFS DWF characterizes the mean square relative displacement (MSRD), and its functional form for the j th coordination shell is given, within Debye approximation, by [22]

$$\sigma_j^2 = \frac{6\hbar}{m\omega_D} \left[\frac{1}{4} + \left(\frac{T}{\theta_D} \right)^2 \int_0^{\theta_D/T} \frac{x}{e^x - 1} dx \right] - \frac{6\hbar}{m\omega_D} \left[\frac{1 - \cos(q_D R_j^0)}{2(q_D R_j^0)^2} + \left(\frac{T}{\theta_D} \right)^2 \int_0^{\theta_D/T} \frac{(\theta_D/q_D R_j^0 T) \sin(q_D R_j^0 T x / \theta_D)}{e^x - 1} dx \right]. \quad (4)$$

Here, θ_D is the Debye temperature, q_D is the Debye wavevector, m is the atomic mass, k_B is the Boltzmann constant, \hbar is Planck's constant and R_j^0 is the interatomic distance for the j th coordination shell. The values of $\Delta\sigma^2$ calculated from (4) are shown for $\theta_D = 250$ K, 300 K, 350 K and 400 K by the dashed lines in figure 7. These values roughly reproduce the experimental results. The values of θ_D that best reproduce the experimental result are 410 ± 40 K, 380 ± 20 K, 325 ± 20 K and 295 ± 15 K for $\theta_i = 20^\circ$, 60° , 75° and 80° , respectively. The θ_D -value for bulk titanium has been reported to lie in the range 342–420 K [17], which is in good agreement with those for $\theta_i = 20^\circ$ and 60° .

We now compare the EELFS θ_D -values estimated above with the effective Debye temperature obtained from the LEED study of the Ti(0001) surface [17]. Since both EELFS and LEED use electrons as a probe, we can discuss the θ_D -values in terms of the penetration depth of the electrons. Figure 8 shows a comparison of the EELFS θ_D -values and the LEED θ_D -values. The range in which the reported Debye temperature of the bulk titanium lies is also indicated by the dashed lines. The estimated EELFS θ_D -value is consistent with the LEED θ_D -value in that both increase as the penetration depth increases. We can observe, however, the tendency of the EELFS θ_D to deviate to larger values at small penetration depths.

With regard to the similarity of the results for the EELFS θ_D and the LEED θ_D mentioned above, we should note the following. It has been reported that the EELFS DWF parametrizes

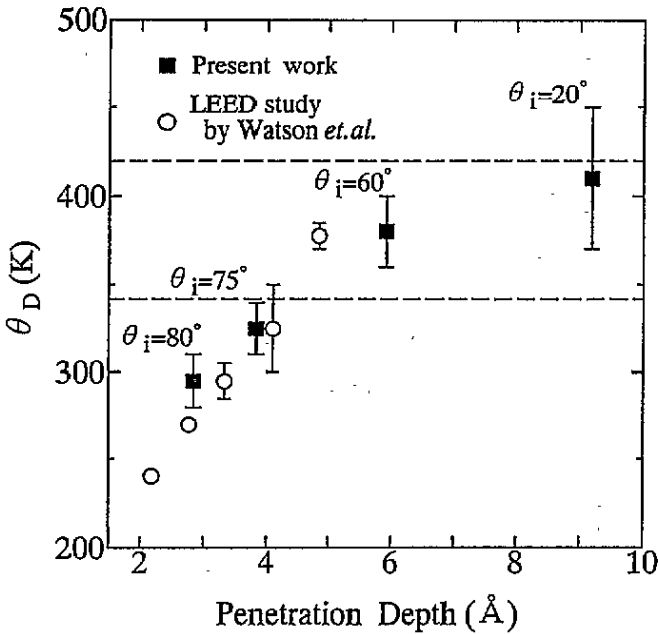


Figure 8. The Debye temperatures estimated from the EELFS DWF at the incidence angles shown and those obtained from the LEED measurement of the Ti(0001) surface [17] plotted against the penetration depth of the electron. The reported Debye temperature for the bulk lies between the two dashed lines.

the MSRD along the direction of the momentum transfer of the incidence electron in the process of the energy loss [13, 15]. Since the direction of momentum transfer cannot be specified under the present experimental conditions, the estimated EELFS θ_D is expected to include the effect from vibrational components both normal and parallel to the surface. In contrast, the LEED θ_D discussed above parametrizes the mean square displacement (MSD) normal to the surface ($\langle u_{\perp}^2 \rangle$). It has been reported that on clean metal surfaces $\langle u_{\perp}^2 \rangle$ is larger than the parallel component of the MSD ($\langle u_{\parallel}^2 \rangle$) [23–25] and as the depth from the surface increases, the difference between $\langle u_{\perp}^2 \rangle$ and $\langle u_{\parallel}^2 \rangle$ rapidly decreases and they approach the value in the bulk [23]. Therefore the EELFS θ_D and the LEED θ_D are expected to coincide with each other at larger penetration depth, i.e. at smaller incidence angles. At small penetration depths, however, because of the larger contribution of the $\langle u_{\parallel}^2 \rangle$ on the surface layer to the EELFS θ_D , the EELFS θ_D is expected to be larger than the LEED θ_D . For a further discussion of the comparison of the EELFS θ_D and the LEED θ_D , detailed knowledge about $\langle u_{\perp}^2 \rangle$ and $\langle u_{\parallel}^2 \rangle$ for various surface planes is needed.

5. Conclusion

The temperature dependence of the EELFS spectra of a polycrystalline titanium surface has been measured with an electron beam at different incidence angles. From the analysis of the measured spectra, we have shown the following. The change in the interatomic distance with depth from the surface is within the experimental error, i.e. less than 0.06 Å. The mean square relative displacement of the titanium atoms is particularly large on the surface layer and is estimated to be more than twice that for the bulk. This result is consistent with that for the LEED measurement.

References

- [1] De Crescenzi M, Chiarello G, Colavita E and Memeo R 1984 *Phys. Rev. B* **29** 3730
- [2] De Crescenzi M, Papagno L, Chiarello G, Scarmozzino R, Colavita E, Rosei R and Mobilio S 1981 *Solid State Commun.* **40** 613
- [3] Lozzi L, Passacantando M, Picozzi P, Santucci S, Diociaiuti M and De Crescenzi M 1992 *Solid State Commun.* **83** 921
- [4] Hitchcock A P and Teng C H 1985 *Surf. Sci.* **149** 558
- [5] De Crescenzi M and Chiarello G 1985 *J. Phys. C: Solid State Phys.* **18** 3595
- [6] Mira F and Noguera C 1987 *J. Phys. C: Solid State Phys.* **20** 3863
- [7] De Crescenzi M, Lozzi L, Picozzi P, Santucci S, Benfatto M and Natoli C R 1989 *Phys. Rev. B* **39** 8409
- [8] Yikegaki T, Shibata H, Takatoh S, Fujikawa T and Usami S 1990 *Phys. Scr.* **41** 185
- [9] De Crescenzi M, Antonangeli F, Bellini C and Rosei R 1983 *Phys. Rev. Lett.* **50** 1949
- [10] Caputi L S, Jiang S L, Amoddeo A and Tucci R 1990 *Phys. Rev. B* **41** 8513
- [11] Idzerda Y U, Williams E D, Einstein T L and Park R L 1987 *Phys. Rev. B* **36** 5941
- [12] Rosei R, De Crescenzi M, Sette F, Quaresima C, Savoia A and Perfetti P 1983 *Phys. Rev. B* **28** 1161
- [13] Tylliszczak T, De Crescenzi M and Hitchcock A P 1988 *Phys. Rev. B* **37** 10664
- [14] De Crescenzi M, Diociaiuti M, Lozzi L, Picozzi P and Santucci S 1987 *Phys. Rev. B* **35** 5997
- [15] Hitchcock A P and Tylliszczak T 1989 *Physica B* **158** 631
- [16] Shih H D, Jona F, Jepsen D W and Marcus P M 1976 *J. Phys. C: Solid State Phys.* **9** 1405
- [17] Watson P R and Mishenko J III 1987 *Surf. Sci.* **186** 184
- [18] Seah M P and Dench W A 1979 *Surf. Interface Anal.* **1** 2
- [19] Denley D, Williams R S, Perfetti P, Shirley D A and Stohr J 1979 *Phys. Rev. B* **19** 1762
- [20] Sirota N N and Zhabko T E 1981 *Phys. Status Solidi* **63** K211
- [21] Stern E A, Sayers D E and Lytle F W 1975 *Phys. Rev. B* **11** 4836
- [22] Beni G and Platzmann P M 1976 *Phys. Rev. B* **14** 1514
- [23] Clark B C, Herman R and Wallis R F 1965 *Phys. Rev.* **139** A860
- [24] Wallis R F and Cheng D J 1980 *Solid State Commun.* **34** 847
- [25] Smith R J, Hennessy C, Kim M W, Whang C N, Worthington M and Xu Mingde 1987 *Phys. Rev. Lett.* **58**